

Synthesis and characterization of xylan-coated magnetite microparticles

Amanda K. Andriola Silva ^{a,b}, Érica L. da Silva ^b, Elquio E. Oliveira ^b, T. Nagashima Jr. ^b, Luiz Alberto L. Soares ^b, Aldo C. Medeiros ^a, José H. Araújo ^c, Ivonete B. Araújo ^b, Artur S. Carriço ^c, E. Sócrates T. Egito ^{a,b,*}

^a Programa de Pós-Graduação em Ciências da Saúde, Universidade Federal do Rio Grande do Norte,
Rua Gal. Gustavo C. de Farias s/n, Natal/RN 59010-180, Brazil

^b Departamento de Farmácia, Universidade Federal do Rio Grande do Norte, Rua Gal. Gustavo C. de Farias s/n, Natal/RN 59010-180, Brazil

^c Departamento de Física Teórica e Experimental, Universidade Federal do Rio Grande do Norte, Campus Universitário, Natal/RN 59072-970, Brazil

Received 11 August 2006; received in revised form 5 October 2006; accepted 9 October 2006

Available online 13 October 2006

Abstract

This work evaluates an experimental set-up to coat superparamagnetic particles in order to protect them from gastric dissolution. First, magnetic particles were produced by coprecipitation of iron salts in alkaline medium. Afterwards, an emulsification/cross-linking reaction was carried out in order to produce magnetic polymeric particles. The sample characterization was performed by X-ray powder diffraction, laser scattering particle size analysis, optical microscopy, thermogravimetric analysis and vibrating sample magnetometry. In vitro dissolution tests at gastric pH were evaluated for both magnetic particles and magnetic polymeric particles. The characterization data have demonstrated the feasibility of the presented method to coat, and protect magnetite particles from gastric dissolution. Such systems may be very promising for oral administration.

© 2006 Elsevier B.V. All rights reserved.

Keywords: Magnetic particles; Gastric dissolution; Polymeric coating; Xylan

1. Introduction

Magnetite particles have been proposed for oral use as magnetic resonance contrast agents and magnetic markers for monitoring gastrointestinal motility (Briggs et al., 1997; Ferreira et al., 2004). Magnetic resonance imaging (MRI) is a non-invasive technique which can provide cross-sectional images from inside solid materials and living organisms (Richardson et al., 2005). MRI has several inherent advantages, such as the lack of radiation exposure, excellent soft tissue contrast, and direct multiplanar capabilities (Kim and Ha, 2003). Advances in MRI, including the implementation of high-performance gradients and the availability of oral contrast agents, have led to an increasing use of MRI in the evaluation of the intestine (Lauenstein et al., 2003), markedly using magnetite particles (Briggs et al., 1997). Magnetite particles were also suggested as

tracers to study the gastrointestinal motility. In fact, such magnetic measurement may be a promising tool in order to evaluate the dynamics of the gastrointestinal tract by monitoring ingested magnetic tracers. Once ingested, the magnetic tracers endow the gastrointestinal tract with a strong magnetic signal. Changes in magnetic signal would be caused by changes in magnetic orientation or volume within the organ due to its motor activity (Ferreira et al., 2004).

Despite the promising properties, magnetite particles dissolve in acid media. The rate of dissolution of oxides is known to increase with increasing hydrogen ion concentration (Schindler, 1991). Gastric juice has an approximate pH of 1, and the normal transit time in the stomach is 2 h (Paulev, 1999–2000; Sinha and Kumria, 2002). The gastric secretions include pepsin, mucus, and hydrochloric acid (HCl) (Paulev, 1999–2000). Therefore, magnetite particle dissolution may take place during the period in which particles pass through the stomach. Such possible particle loss could reduce the signal for MRI or for monitoring gastrointestinal motility, depleting the efficiency of the system.

Regarding pharmaceutical technology, protecting compounds from gastric environment is a key issue. In fact, many approaches have been proposed, namely coating with pH-

* Corresponding author at: UFRN, CCS, Departamento de Farmácia, Rua Praia de Areia Branca 8948, CEP 59094-450, Brazil. Tel.: +55 84 94 31 88 16; fax: +55 843 215 4355.

E-mail address: socrates@digi.com.br (E.S.T. Egito).

sensitive polymers, time-dependent delivery systems, and the use of biodegradable polymers (Sinha and Kumria, 2001). Concerning pH-dependent systems, they exploit the fact that the pH of the human gastrointestinal tract increases progressively from the stomach (pH 1–2) to the intestine (pH 6–8). The polymers used to design such systems should be able to withstand the lower pH values of the stomach in order to protect the compound from the gastric fluid (Chourasia and Jain, 2003). The time-dependent formulations are designed to resist the release of the drug in the stomach with an additional non-disintegration or lag phase. Intestinal release is enabled, and protection from gastric environment is provided (Sinha and Kumria, 2001). The other strategy relies on the resistance of some polysaccharides to the digestive actions of gastrointestinal enzymes. The matrices of polysaccharides are assumed to remain intact in the physiological environment of stomach and small intestine. Once they reach the colon, bacterial polysaccharidases come into play, and degradation of the matrices takes place. Such group of polysaccharides is comprised of amylase, chitosan, pectin, dextran, inulin, chondroitin, xylan, etc. These polymers present a large number of derivatizable groups, a wide range of molecular weights, low toxicity, biodegradability, and high stability (Chourasia and Jain, 2003). Because of the presence of biodegradable enzymes only in the colon, such systems seem to be more suitable with regard to selectivity as compared to the other approaches (Sinha and Kumria, 2001).

Among the colon-degradable polymer cited above, xylan is a very promising one. In fact, it is the most common hemicellulose, and represents more than 60% of the polysaccharides existing in the cell walls of corn cobs (Ebringerova et al., 1992). It is considered the second most abundant biopolymer in the plant kingdom. Its chemical structure is mainly composed of D-glucuronic acid, L-arabinose and D-xylose in the approximate ratio of 2:7:19 (Ebringerova et al., 1994). The aim of this work was to develop xylan-coated magnetic microparticles in order to protect magnetite from gastric dissolution.

2. Materials and methods

2.1. Materials

Ferric chloride hexahydrate (Synth Chemical, Brazil; 97%), ferrous sulphate heptahydrate (Synth Chemical, Brazil; 99%), sodium hydroxide (Vetec Chemical, Brazil; 98%), hydrochloric acid (Vetec Chemical, Brazil; 37%), chloroform (Vetec Chemical, Brazil; 99%), cyclohexane (Vetec Chemical, Brazil; 99%), terephthaloyl chloride (Sigma Chemical, German; 99%), and sorbitan triesterate (Aldrich Chemical, USA) were used as received from manufacturers. Xylan was extracted from corn cobs (Garcia et al., 2001).

2.2. Methods

2.2.1. Synthesis of magnetic particles (MP)

The set-up used to synthesize magnetic particles was based on coprecipitation method (Kim et al., 2001; Koneracka et al., 2002; Massart, 1981). Solutions of ferric chloride and ferrous

sulphate were prepared as a source of iron by dissolving the respective chemicals in a 0.4 M HCl solution under vigorous stirring using a mechanical stirrer (IKA RW-20, Germany) at 960 rpm at room temperature (25 °C). As a second step, solutions were combined and a homogenous mixture of FeCl_3 (0.1 M) and FeSO_4 (0.05 M) was formed. An aqueous dispersion of particles was obtained just after adding 9 ml of the mixture of ferrous and ferric salts drop-wise into 450 ml of NaOH 1M under sonication (Unique USC 1800, 40 kHz, Brazil) and vigorous mechanical stirring at 960 rpm (IKA RW-20, Germany) for 30 min at room temperature (25 °C). For such synthesis, the chemical reaction is expected as follows:



2.2.2. Production of polymeric magnetic particles (PMP)

In the following step, 0.115 g of xylan was dissolved in 9.2 mL of 0.6 M NaOH under vigorous stirring at room temperature. The magnetic suspension [0.025 g/mL], previously neutralized, was sonicated for 40 min and 3 mL of this suspension was added into the xylan solution. Emulsification was then carried out in 30 mL of chloroform: cyclohexane [1:4 (v/v)] containing 5% (w/v) sorbitan triesterate. By adding 40 mL of a 5% (w/v) terephthaloyl chloride solution, interfacial cross-linking reaction took place under vigorous stirring. PMP were separated by centrifugation and several washes.

2.2.3. Size and morphology studies

The mean diameter of MP and PMP was examined using a laser scattering particle size analyzer (Cilas, 920L, France). The technique is based on the principle of Fraunhofer diffraction to determine the particle size of diluted suspensions. Samples were pretreated using a dispersing agent (sodium hexametaphosphate) to inhibit flocculation, and then dispersed and homogenized.

Morphology analysis of PMP was conducted by microscopy on a scanning electron microscope (XL 30 ESEM, Philips, The Netherlands). One drop of the MP/PMP suspension and one drop of water were added on a lamina surface, and investigated at 10×, 40× and 100× magnification.

2.2.4. X-ray analysis

The structural properties of MP were characterized by X-ray powder diffraction (XRPD), which was carried out in an X-ray diffractometer (Shimadzu, XRD-6000, Japan). Representative powder samples were analyzed in the range $10^\circ < 2\theta < 80^\circ$ by using the $\text{K}\alpha$ line Cu as a radiation source with wavelength 1.54056 Å.

2.2.5. Thermogravimetric analysis

The magnetite content in the polymeric microparticles was assessed by thermogravimetric analysis (Shimadzu TGA-50H, Japan). PMP, MP and a sample produced just like PMP except for the magnetite content (polymeric particles, PP) were analyzed. The powder samples were obtained by drying aqueous suspensions using the same method reported above. During analysis

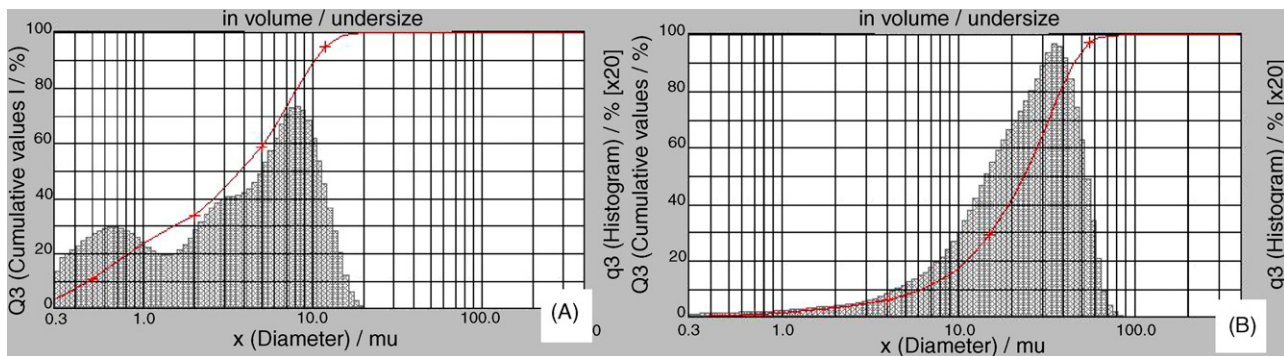


Fig. 1. Size distribution of magnetic particles (A) and polymeric magnetic particles (B).

the sample was heated in an air stream with a heating rate of $10^{\circ}\text{C min}^{-1}$ from room temperature up to 1000°C .

2.2.6. Magnetization measurements

Magnetization measurements on powder MP and PMP samples were performed using a homemade vibrating sample magnetometer (VSM), previously calibrated with nickel. Representative powder samples were obtained after MP and PMP suspensions were dried at 100°C for 3 h on Petri dishes. Magnetization versus applied field was measured at room temperature for all samples. The magnetometer was calibrated with nickel. Analyses were carried out using a maximum applied field of 1.17 T. The field was swept from 0 to 1.17 T, then through 0 to 1.17 T, and finally, through 0 to 1.17 T.

2.2.7. Dissolution study

As iron oxide undergoes proton-assisted dissolution, this study was performed at the most acid gastrointestinal pH. Magnetite dissolution at gastric pH was determined in vitro for MP and PMP samples, both containing 18.94 mg of magnetite. A dissolution apparatus (Sotax AT 7, Allschwil/Basel, Switzerland) with paddles was employed to carry out all of the tests. The dissolution medium, experimental temperature, and paddle speed were 1000 ml of 0.1 M HCl, $37 \pm 0.1^{\circ}\text{C}$, and 100 rpm, respectively. At regular intervals of time, 15 ml samples were withdrawn. Free iron was assessed spectrophotometrically

(Cary-Varian 1 E UV-vis spectrophotometer) at 512 nm from a standard curve, according to phenanthroline method (Gary, 1994).

3. Results and discussion

3.1. Size and morphology studies

Laser diffraction was employed to analyze the size distribution of MP and PMP (Fig. 1). The mean diameter was calculated by "The Particle Expert" software from Cilas equipment, and consisted of the De Brouckere mean diameter, also called $D[4,3]$. Concerning MP, it was found to be $4.88 \pm 1.77 \mu\text{m}$. It was also determined that 90%, 50% and 10% of the sample was smaller than 9.81 ± 1.78 , 2.80 ± 0.69 and $0.36 \pm 0.03 \mu\text{m}$, respectively. The size of the MP was not uniformly distributed around the median value. Instead, it showed a tendency towards a bimodal distribution with a left sided tail. The mean diameter of PMP was found to be $25.26 \pm 0.42 \mu\text{m}$. It was also determined that 90%, 50% and 10% of the sample was smaller than 45.52 ± 0.66 , 23.76 ± 0.54 and $6.26 \pm 0.14 \mu\text{m}$, respectively. The polymeric coating process produced changes in the particle size distribution, and the MP bimodal distribution was replaced by a unimodal one. Additionally, PMP was nearly five-fold larger, suggesting that the polymeric coating involved more than one particle, consisting of multi-core/shell structures. Addi-

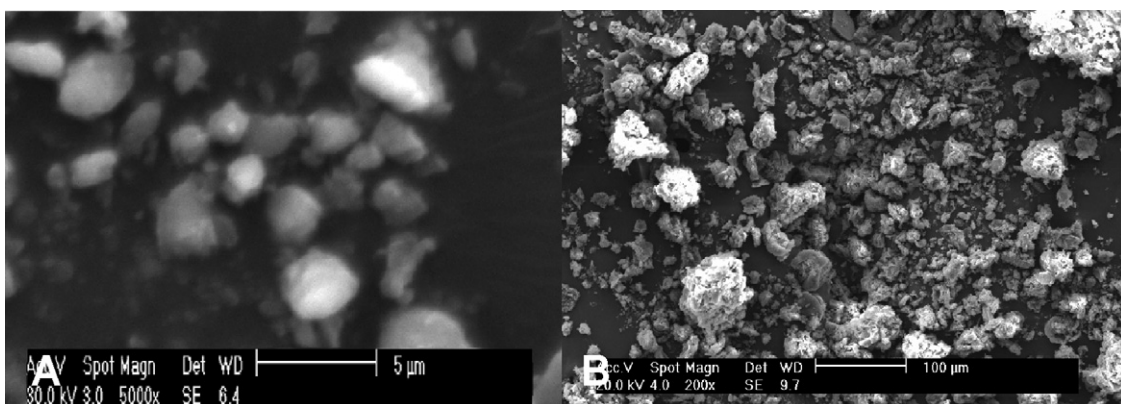


Fig. 2. Scanning electron microscopy images of magnetic particles (A) and polymeric magnetic particles (B).

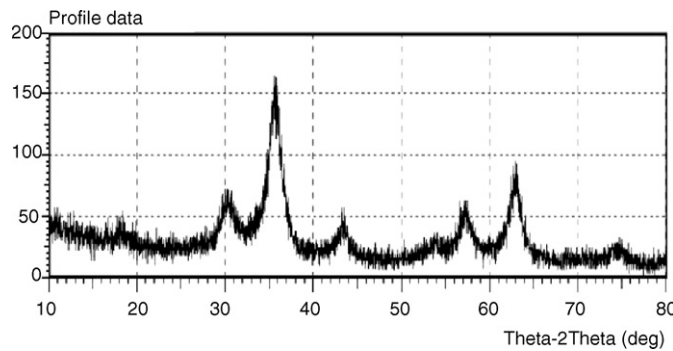


Fig. 3. X-Ray powder diffraction patterns of magnetic particles.

tionally, the PMP were found to be roughly spherical in shape (Fig. 2).

The span index was used to analyze the polydispersity in the particle size distribution. It is defined as $(D90 - D10)/D50$, where $D10$, $D50$, and $D90$ are the respective particle sizes at 10, 50, and 90% cumulative percentage undersize. The span index of MP was 3.375, indicating high polydispersity. For PMP, the polydispersity was decreased markedly down to 1.652.

3.2. X-ray analysis

According to XRPD patterns, as shown in Fig. 3, magnetite was the dominant phase in the analyzed sample, with a primary scattering peak at around $2\theta = 35^\circ$ (Chen and Hu, 2003). The XRPD patterns analysis suggested the absence of ferric hydroxide that would produce a primary peak at $2\theta = 26.38^\circ$. Additionally, no peaks of other compounds, such as goethite ($2\theta = 21.22^\circ$) and hematite ($2\theta = 31.15^\circ$) were observed.

3.3. Thermogravimetric analysis

Thermogravimetric analyses were carried out for PMP, MP and PP (Fig. 4).

Concerning MP, there was no weight loss up to 1000°C , except for a likely water loss in the sample. In fact, no thermal event is expected for magnetite particles in the temperature range of TGA (Pan et al., 2005).

Regarding PP, weight loss took place mainly in the temperature range of $230\text{--}500^\circ\text{C}$. At 450°C , nearly all the sample mass had been already decomposed (97.4%).

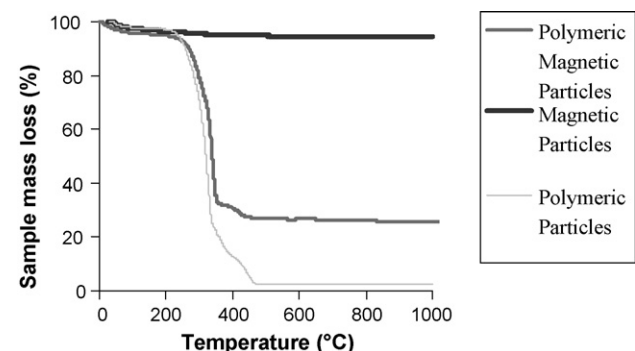


Fig. 4. Thermogravimetric analysis of polymeric magnetic particles, magnetic particles and polymeric particles.

Concerning the PMP, TGA curve revealed that the thermal events occurred in two temperature ranges: $25\text{--}100$ and $230\text{--}500^\circ\text{C}$. In the first one, the decrease of weight was about 5%, which could be attributed to desorption of water. In the second zone, weight loss was nearly 70%. It could be attributed to the polymeric coating, as PP weight loss was observed in the same temperature range. At 1000°C , the remaining mass was about 25%, attributed to magnetite content. Therefore, polymer coating/magnetite ratio was 14:5. Considering such data and the initial polymer/magnetite mass ratio, encapsulation efficiency was about 66%.

3.4. Magnetization measurements

The results shown in Fig. 5 indicated that MP readily displayed magnetization when subjected to a magnetic field. It was found that there was no remanent magnetization ($M=0$ for $H=0$) suggesting that MP was superparamagnetic. However, considering the particle size distribution (Fig. 1), there should be a nett magnetization in the absence of external field. One possible mechanism for this unique form of superparamagnetism is the independent thermal fluctuation of small ferrimagnetic domains inside the particles. The boundaries of the small crystallites within the particles may contain lattice defects that impede the propagation of the magnetic order (Silva et al., in press). The same magnetic properties were observed for the PMP. Although the PMP consisted of multi-core/shell structures, as mentioned above, such additional agglomeration did not change the superparamagnetic properties of the system. Concerning saturation magnetization, it was found to decrease for PMP as compared

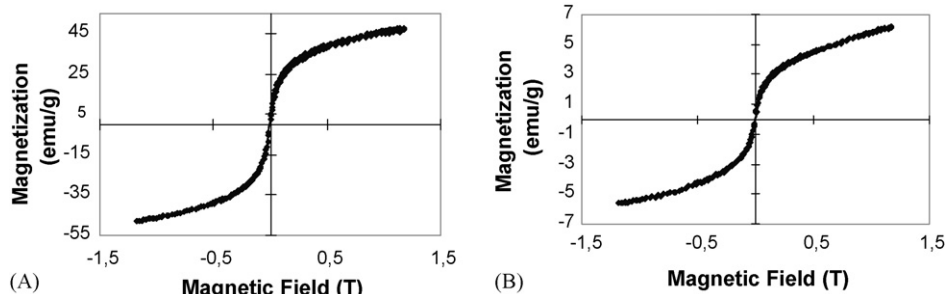


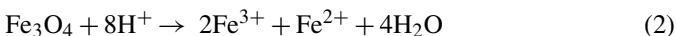
Fig. 5. Magnetization curves of magnetic particles (A) and polymeric magnetic particles (B).

to MP. However, such decrease in the saturation magnetization is expected to take place when the powders are polymer-coated (Ramanujan and Yeow, 2005) since the measurement unit is mass-related.

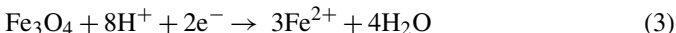
3.5. Dissolution study

Magnetic particles synthesized by coprecipitation are macroanions. Electric charges are due to specific adsorption of the amphoteric hydroxyl group, which leads to superficial negative charges in the alkaline medium and positive charges in the acidic one (Bacri et al., 1990). Superficial acid–base reactivity plays an important role in understanding the mechanisms of magnetite dissolution. Such mechanisms comprise protonation, reduction or complexation (Schindler, 1991).

Regarding protonation mechanism, protons promote the dissolution process by protonating OH groups on the mineral surface. Such process contributes to a weakening of the Fe–O bond (van Oorschot and Dekkers, 2001). As this bond is weakened, iron is released into the solution according to the equation below (Keny et al., 2005). The rate of dissolution of oxides is known to increase with increasing hydrogen ion concentration (Schindler, 1991):



Concerning the second mechanism, the reduction of Fe(III) to Fe(II) brings about a large increase in the rate of dissolution. The origin of this increase is the greater lability of Fe(II)–O bonds as compared to Fe(III)–O bonds (Baumgartner et al., 1983). This mechanism is called reductive dissolution and depends on the pH, temperature and redox potential (Al-Mayouf and Al-Arifi, 2005), according to equation (Keny et al., 2005):



Concerning complexation mechanism, it comprises three distinct steps (Panias et al., 1996): adsorption of organic ligands on the iron oxide surface, non-reductive dissolution and reductive dissolution. All these mechanisms have in common that they are surface controlled and the dissolution rate depends on the concentration of the dissolution-promoting species on the surface (Suter et al., 1991).

Considering the mechanism involved in the dissolution of magnetite particles in the stomach, protonation may play an utmost important role since gastric juice has an approximate pH of 1 (Paulev, 1999–2000). However, the presence of food in the stomach may influence magnetite dissolution by a different mechanism. For instance, ascorbic acid, which is a reducing ligand, act as an electron donor reducing the surface iron(III) sites. As a consequence, soluble iron(II) is released (Suter et al., 1991).

Concerning MP sample, 28.47% of the magnetite content was dissolved by the 120 min (Fig. 6). MP presented the highest dissolution rate during the early beginning of the dissolution test, 9.27% of dissolution during the first 15 min. Such effect may be due to the left-sided tail in MP size distribution. As it can

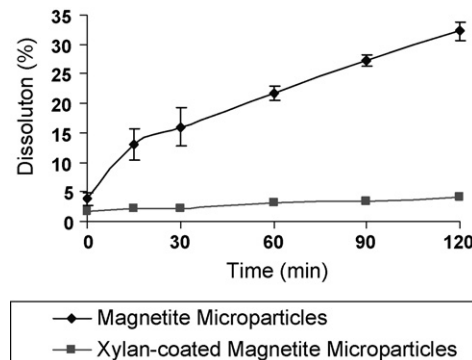


Fig. 6. Dissolution profile of magnetic particles and polymeric magnetic particles.

be expected, iron oxide dissolution rate in acid pH is dependent on particle size (Chastukhin et al., 2003). Therefore, the fraction of small particle size probably underwent dissolution first. Dissolution presented then an almost linear pattern from 15 to 120 min ($R^2 = 0.9991$). Regarding PMP sample, only 2.3% of the magnetite content was dissolved by 120 min. In this sample, particles were more uniformly distributed around the median value. Therefore, a nearly uniform dissolution took place, presenting a linear correlation coefficient of 0.9681.

Comparing the different dissolution profiles, a clear change in the slope on magnetite dissolution curve is observed for PMP. Differences in dissolution profiles may be ascribed to a combination of factors. Firstly, as expected, xylan did not dissolve at gastric pH. Secondly, nearly all particles were polymer-coated. Last but not least, coating was thick and imporous enough to create a quite impermeable layer to the surrounding acid solution.

4. Conclusions

In this work, xylan-coated magnetic microparticles were developed. At gastric pH, PMP scarcely underwent dissolution compared to MP. Therefore, it was shown that xylan coating did shield magnetite from the gastric pH. Concerning the administration of magnetic systems by the oral route, this was a striking result. Gastric dissolution and the consequent particle loss could reduce the signal for MRI or for monitoring gastrointestinal motility, depleting the efficiency of the system. Altogether, it can be considered that xylan-coated magnetic microparticles may be very promising for oral administration.

Acknowledgements

This work was funded by the grant no. 47836/01-7-NV from CNPq, and partially funded by BNB and by Capes, Brazil.

References

- Al-Mayouf, A.M., Al-Arifi, A.S.N., 2005. Reductive dissolution of magnetite in ethylenediaminedisuccinic acid solutions. Desalination 181, 233–241.
- Bacri, J.C., Perzynski, R., Salin, D., Cabuil, V., Massart, R., 1990. Ionic ferrofluids—a crossing of chemistry and physics. *J. Magn. Magn. Mater.* 85, 27–32.

Baumgartner, E., Blesa, M.A., Marinovich, H.A., Maroto, A.J.G., 1983. Heterogeneous electron-transfer as a pathway in the dissolution of magnetite in oxalic-acid solutions. *Inorg. Chem.* 22, 2224–2226.

Briggs, R.W., Wu, Z., Mladinich, C.R.J., Stoupis, C., Gauger, J., Liebig, T., et al., 1997. In vivo animal tests of an artifact-free contrast agent for gastrointestinal MRI. *Magn. Reson. Imaging* 15, 559–566.

Chastukhin, A.E., Izotov, A.D., Gorichev, I.G., Kutepov, A.M., 2003. Analysis of Fe_2O_3 and Fe_3O_4 dissolution kinetics in terms of the chain mechanism model. *Theor. Found. Chem. Eng.* 37, 398–406.

Chen, J.C., Hu, C.C., 2003. Quantitative analysis of YIG, YFeO_3 and Fe_3O_4 in LHPG-grown YIG rods. *J. Cryst. Growth* 249, 245–250.

Chourasia, M.K., Jain, S.K., 2003. Pharmaceutical approaches to colon targeted drug delivery systems. *J. Pharm. Pharm. Sci.* 6, 33–66.

Ebringerova, A., Hromadkova, Z., Alfoldi, J., Berth, G., 1992. Structural and solution properties of corn cob heteroxylans. *Carbohydr. Polym.* 19, 99–105.

Ebringerova, A., Hromadkova, Z., Kacurakova, M., Antal, M., 1994. Quaternized xylans—synthesis and structural characterization. *Carbohydr. Polym.* 24, 301–308.

Ferreira, A., Carneiro, A.A.O., Moraes, E.R., Oliveira, R.B., Baffa, O., 2004. Study of the magnetic content movement present, in the large intestine. *J. Magn. Magn. Mater.* 283, 16–21.

Garcia, R.B., Nagashima, T., Praxedes, A.K.C., Raffin, F.N., Moura, T., do Egito, E.S.T., 2001. Preparation of micro and nanoparticles from corn cobs xylan. *Polym. Bull.* 46, 371–379.

Gary, D.C., 1994. Analytical Chemistry, vol. 5. John Wiley & Sons, Inc.

Keny, S.J., Kumbhar, A.G., Venkateswaran, G., Kishore, K., 2005. Radiation effects on the dissolution kinetics of magnetite and hematite in EDTA- and NTA-based dilute chemical decontamination formulations. *Radiat. Phys. Chem.* 72, 475–482.

Kim, D.K., Zhang, Y., Voit, W., Rao, K.V., Muhammed, M., 2001. Synthesis and characterization of surfactant-coated superparamagnetic monodispersed iron oxide nanoparticles. *J. Magn. Magn. Mater.* 225, 30–36.

Kim, K.W., Ha, H.K., 2003. MRI for small bowel diseases. *Semin. Ultrasound CT MRI* 24, 387–402.

Koneracka, M., Kopcansky, P., Timko, M., Ramchand, C.N., 2002. Direct binding procedure of proteins and enzymes to fine magnetic particles. *J. Magn. Magn. Mater.* 252, 409–411.

Lauenstein, T.C., Schneemann, H., Vogt, F.M., Herborn, C.U., Ruhm, S.G., Debatin, J.F., 2003. Optimization of oral contrast agents for MR imaging of the small bowel. *Radiology* 228, 279–283.

Massart, R., 1981. Preparation of aqueous magnetic liquids in alkaline and acidic media. *IEEE Trans. Magn.* 17, 1247–1248.

Pan, B.F., Gao, F., Gu, H.C., 2005. Dendrimer modified magnetite nanoparticles for protein immobilization. *J. Colloid Interface Sci.* 284, 1–6.

Panias, D., Taxiarchou, M., Paspaliaris, I., Kontopoulos, A., 1996. Mechanisms of dissolution of iron oxides in aqueous oxalic acid solutions. *Hydrometallurgy* 42, 257–265.

Paulev, P.-E., 1999–2000. Gastrointestinal function and disorders. In: Paulev, P.-E. (Ed.), *Textbook in Medical Physiology And Pathophysiology*. Copenhagen Medical Publishers, Copenhagen.

Ramanujan, R.V., Yeow, Y.Y., 2005. Synthesis and characterisation of polymer-coated metallic magnetic materials. *Mater. Sci. Eng. C* 25, 39–41.

Richardson, J.C., Bowtell, R.W., Mader, K., Melia, C.D., 2005. Pharmaceutical applications of magnetic resonance imaging (MRI). *Adv. Drug Delivery Rev.* 57, 1191–1209.

Schindler, P.W., 1991. A solution chemists view of surface-chemistry. *Pure Appl. Chem.* 63, 1697–1704.

Silva, A.K.A., Soares, L.A.L., Carriço, A.S., Egito, E.S.T., Development of superparamagnetic microparticles for biotechnological purposes (SUBMITTED). *Chemical & Pharmaceutical Bulletin*.

Sinha, V.R., Kumria, R., 2001. Polysaccharides in colon-specific drug delivery. *Int. J. Pharm.* 224, 19–38.

Sinha, V.R., Kumria, R., 2002. Binders for colon specific drug delivery: an in vitro evaluation. *Int. J. Pharm.* 249, 23–31.

Suter, D., Banwart, S., Stumm, W., 1991. Dissolution of hydrous iron(III) oxides by reductive mechanisms. *Langmuir* 7, 809–813.

van Oorschot, I.H.M., Dekkers, M.J., 2001. Selective dissolution of magnetic iron oxides in the acid–ammonium oxalate/ferrous iron extraction method. I. Synthetic samples. *Geophys. J. Int.* 145, 740–748.